Variable NTE behaviour in siliceous and Al substituted Cu/SSZ-13

Daniel Silva Nunes,[a,*] Ian Robinson,[b] Scott Woodley,[a] Misbah Sarwar,[b] Paul Collier,[b] and Richard Catlow[a]

a) University College London
b) Johnson Matthey PLC
* uccasil@ucl.ac.uk

We report a computational investigation of the effect of different Al distributions on the Negative Thermal Expansion (NTE) of Cu/SSZ-13. All systems investigated were found to display NTE behaviour within the temperature range studied (200 K – 600 K), with different Al configurations leading to different NTE magnitudes. As the concentration of these Al increases in the zeolitic framework (*i.e.* further reducing the Si:Al ratio) the NTE behaviour was found also to increase.

Zeolites are microporous silicates that have supported a plethora of chemical applications, ranging from catalysis to molecular sieving. The diversity of applications is enhanced by the great variety of topologies found within this class of materials, with 234 topologically distinct zeolitic frameworks reported to date.[1] Zeolites are now widely used in auto-exhaust catalysis, especially for the removal of polluting nitrogen oxides (NOx). Currently, zeolites based on the *Chabazite* (CHA) framework are increasingly employed as commercial de-NOx catalysts.[2]

Recently, it was established that copper substituted SSZ-13 (Cu/SSZ-13) had excellent conversion rates of NO_x within the temperature ranges found within the *modus operando* of automotive engines, involving selective catalytic reduction (SCR) of NO_x, also known as the *de*NO_x. Although a number of versions of this reaction have been proposed, Cu/SSZ-13 is known to produce the best performance when ammonia (NH_3), supplied to the engine system via urea, for the NH_3*-SCR* of NO_x. The reasons why the CHA framework is so successful in this reaction include the fact that it is a small pore zeolite, with a suitable size for the molecules involved in the conversion mechanism. High thermal stability is also important, since some zeolite frameworks start degrading at high temperatures via de-alumination, in which the Al found in the framework detaches itself to form alumina nanoclusters. Although CHA displays these advantages for the NH_3*-SCR* of NO_x, it has been reported that at relatively high humidity and low temperature, the rates of conversion of NOx during the NH3-SCR go down drastically. Leistner *et al.* argue that the lack of activity under these environmental conditions is due to a structural rearrangement of the Cu^{2+} active site.[3] However, the mechanisms involved in this de-activation takes are not understood in detail. Thus, it is the aim of this publication to bring light to one of the possible basic mechanisms via which this deactivation may be taking place; namely the effect of temperature on the framework and how different Al environments lead to a change in the structural geometry of the unit cell and thus possibly distorting the Cu^{2+} active site.

The majority of materials display an overall volume increase when heated – *ie.* having positive thermal expansion (PTE). Interestingly, however, some materials contract upon heating, showing negative thermal expansion (NTE). Although PTE is known to occur mostly due to the asymmetry of the interatomic potential well, NTE has been proposed to arise due to a number of mechanisms. As the work here presented concentrates on zeolites, we will focus on the mechanism operative in these materials: the rigid unit mode (RUM) model, detailed accounts of which are available .[4,5] The RUM, firstly presented by Sleight, proposes that the repulsion between adjacent oxygens in metal oxides, where the *M-O* bond strength is strong, promotes the preponderance of transverse vibrational modes, related to the *M-O-M* linkages, over longitudinal ones. These transverse modes ultimately lead to a rotation about the *M-O-M* hinges (equivalent to a rotation of the structural polyhedral).

The siliceous version of the CHA zeolite has been shown to display NTE behaviour in previous studies.[6] It is an orthorhombic structure, with the *R3m* space group with lattice parameters of *a* = *b* = 13.5 Å and c = 14.5 Å. With regards to the location of the active Cu extra-framework ion, it known to have two preferred sites; co-planar to the six-membered ring (6mr) and in the eight-membered ring (8mr), slightly deviated towards the larger pore.

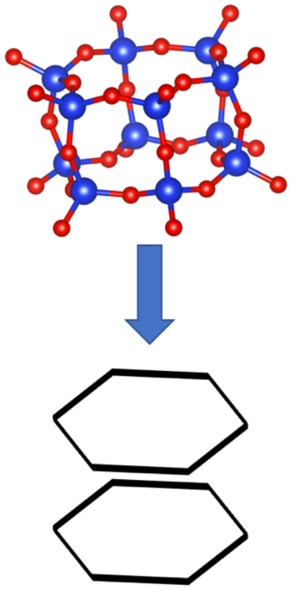

Figure 1. A depiction of the six membered double ring found in the *CHA* framework and its conversion to the model used for the purposes of aluminium substitution in this work.

NTE is an intriguing effect and the factors controlling its magnitude are often poorly understood. In this paper, we aim to improve our fundamental understanding of NTE behaviour by employing simulation techniques to probe the effect and examining its variation as a function of Al loading in the zeolite.

Methodology: The General Utility Lattice Package (GULP) code was used to calculate free energy minimised structures as a function of temperature. The CHA framework was obtained from the International Zeolite Associate database and a range of Al concentrations and distributions in framework sites were generated as discussed in greater detail below. The GULP code uses interatomic potential models in order to describe the interactions between the constituents of the zeolitic framework. For the case of the Si-O interactions, those modelled by Sanders *et al*. were used.[7] While for the Al-O and O-O interactions, the potentials fitted by Catlow et al. were chosen.[8]

These potentials have been used in the past and have been successful in predicting a number of properties in the zeolites.[9] The reliability of these potentials has been benchmarked by using them to compute the thermal expansion coefficient (CTE) of alpha-quartz. For systems discussed in the literature [name examples], the potentials correctly predicted a positive expansion behaviour.

As discussed in the Introduction, this study aims to reveal the effects of different Al chemical environments in the zeolitic frameworks on their NTE behaviour, to achieve which, five different configurations of Al were probed. These same configurations have been studied in the past by Gölt *et al*.[10] An illustration is given in **Figure 2**. With regard to the position of the Cu^{2+} extra-framework ion, it is known to be present in two sites: (i) co-planar to one of the *6mr* and (ii) in the *8mr*. To study the reliability of these chosen potentials within the CHA framework, the Cu^{2+} was sited around the Brønsted acidic sites which yielded four possible positions: 1) co-planar to the 6MR; 2) inside the 6 double ring; 3) in co-planar to the 8MR and 4) protruding into the larger pore. The used representation of a section of the *CHA* framework is seen in **Figure 1**.

For each structure free energy optimisation was undertaken, employing the Broyden-Fletcher-Goldfarb-Shanno (BFGS) optimisation technique, which has also been routinely used in zeolite modelling studies.[9] A temperature of 0 K was used during the initial optimisation process, ie a static lattice (SL) calculation with energy minimisation. For all Al configurations, the Cu^{2+} extra-framework ion was found to be less stable in the 4MR, 6DR and when protruding into the larger cavity. The ion either migrated to the 6MR or to the 8MR; which agrees with previous studies.[2] The most stable configuration for the Cu was in the *6mr* ; again, concurring to what has been reported previously.[2,10] Taking into account these results, the models of the five different Al pairing configurations containing the Cu in the *6mr* were put through to the next stage: here each system was probed at temperatures ranging from 200 K to 600 K (which are the temperatures that may be experienced by these zeolites during the NH3-SCR of NOx), in 100 K steps. In order to differentiate between structures throughout this text, the following naming system found in **Table 1** was used.

Table 1 | Notation used for different Al distributions

System	Code
SSZ-13	Z_0
SSZ-13, Al pair 1	Z_1
SSZ-13, Al pair 2	Z_2
SSZ-13, Al pair 3	Z5
SSZ-13, Al pair 4	Z3
SSZ-13, Al pair 5	Z4

Energetics of SSZ-13 and Al pairs: After minimising the energy of each of the structures at 0K, it was found that, with the exception of Z_2, all the optimised systems yielded a gradient norm (Gnorm) below the established threshold of 1 x 10^{-4} NÅ^{-1}. The lowest energy zeolitic system was Z_0 at - 47.958 kJmol^{-1}, followed by Z_2, Z4, Z5 and Z3 at - 47.364 kJmol^{-1}, - 47.356 kJmol^{-1}, - 47.355 kJmol^{-1} and - 47.354 kJmol^{-1}, respectively. The associated Gnorms for structure solutions may be found on **Supplement 1**. An illustration of these energy and Gnorms is shown for each of the structures in **Figure 2**. Since the Gnorm of Z_2 was above threshold, this Al pairing configuration will subsequently be disregarded, and thus only Z0, Z1, Z5, Z3 and Z4 will have data on structural temperature effects.

NTE behaviour of siliceous and Al substituted SSZ-13: All structures were found to display NTE behaviour throughout the sampled temperature range. The CTE on the unit cell volume of this system was found to be -1.98 ± 0.01 x 10^{-5} K^{-1} for Z_0; (the linear regression produced an R^2 of 1.00.) The CTE on the lattice parameters of Z_0 was -0.83 ± 0.02 x 10^{-5} K^{-1} for lattice parameter *a*, -0.83 ± 0.02 x 10^{-5} K^{-1} for b and -0.33 ± 0.03 x 10^{-5} K^{-1} for *c*. The lattice parameter ratios were found to be 1.00 and 0.93 for a/c and b/c throughout the entire temperature range. For the remaining structures, only the CTE of the unit cell volume (and associated $R^{2)}$ will be discussed. Details of the results on the CTE of the lattice parameters, as well as on the lattice parameters ratios on **Table 2** and **3**. The latter was found to be invariant of the temperature and thus only one value is given for each of the ratios. With regard to the volumetric CTE of Z_1 to

Table 2 | A list of the computed CTEs of each system of the published literature.

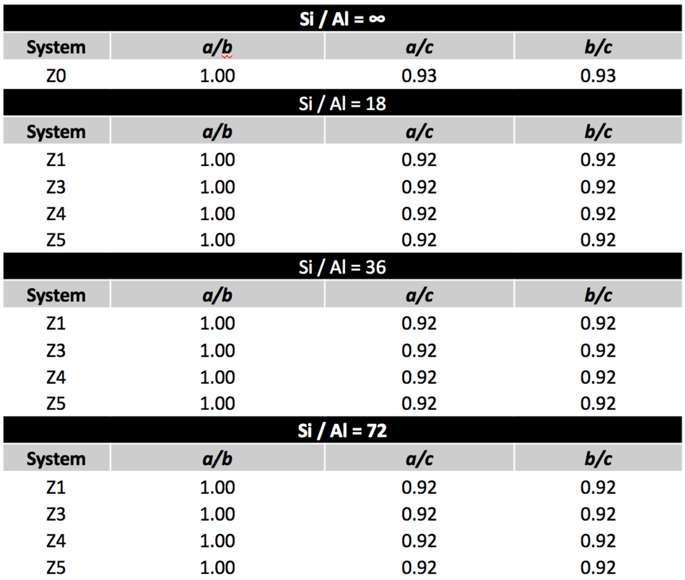

Si / Al = ∞			
System	***a/b***	***a/c***	***b/c***
Z0	1.00	0.93	0.93
Si / Al = 18			
System	***a/b***	***a/c***	***b/c***
Z1	1.00	0.92	0.92
Z3	1.00	0.92	0.92
Z4	1.00	0.92	0.92
Z5	1.00	0.92	0.92
Si / Al = 36			
System	***a/b***	***a/c***	***b/c***
Z1	1.00	0.92	0.92
Z3	1.00	0.92	0.92
Z4	1.00	0.92	0.92
Z5	1.00	0.92	0.92
Si / Al = 72			
System	***a/b***	***a/c***	***b/c***
Z1	1.00	0.92	0.92
Z3	1.00	0.92	0.92
Z4	1.00	0.92	0.92
Z5	1.00	0.92	0.92

Z_5, the values were found to be -1.49 ± 0.02 x 10^{-5} K^{-1}, -1.71± 0.01 x 10^{-5}, -1.89 ± 0.02 x 10^{-5} K^{-1}, respectively. These results were obtained for Si:Al ratios of 18, 36 and 72; although the remaining discussion will focus on the results for a Si:Al ratio of 18. Details of the calculated values are given in **Table 3**, while we refer to **Table 2** for information on the variability of the lattice parameters as a function of these Si:Al ratios, as well as a function of the Al pairing configuration. The expansion behaviour for each of the systems was found to be anisotropic for all the aluminous frameworks (Z1 – Z5) and isotropic for the purely siliceous case (Z0).

Discussion: The results from our calculations showed that, regarding energies, the substituted frameworks were similar. The variability was of the order of 10^{-3} kJ mol^{-1}; with the Z_1 framework the most stable. These results agree with the DFT results of Gölt *et al*;[10].The fact that Z_2 produced such a larger Gnorm when compared to the other structures may have been due to the fact this is the case for when the Al pairs are closest to each other. According to Löwenstein's rule, Al-O-Al linkages should be expected in zeolitic frameworks. For this reason, it was proposed that this particular Al pairing configuration should be left out from LD procedure.

The zeolite frameworks studied in the lattice dynamics calculations all display NTE behaviours. This accords with expectations: a small number of Al substitutions should not modify the overall thermal behaviour of the framework. When compared with the results obtained by Woodcock and by Martinez (whose experimental data show NTE behaviour for SSZ-13 under these conditions), the calculated value is found to lie between their experimental results. Given that the different experiments diverge by as much as 0.74 K^{-1}, the calculated results appear to be acceptable.

Considering the frameworks with the substituted Al ions, an increase in the temperature, within the same temperature range, also led to a contraction of the unit cell and of all three lattice parameters in a monotonic manner. However, our results show some dependence of the CTE on the type of Al pairing configuration. As shown in **Table 3**, the values for the CTE (both volumetric and those for the lattice parameters) not only change on comparing between structures, but also change within the same configuration at different Si:Al ratios. As the Al content decreases, the unit cell volume decreases, which is to be expected since, as the Si/Al ratio increases the behaviour of the system will converge on that of Z_0 (**Figure 3**). We should note that for $Z_{0,}$ the unit cell contraction was found to be isotropic, whereas for all the other cases it was anisotropic. To preserve *R3m* space group symmetry, one would expect a and b to expand at the same rate.

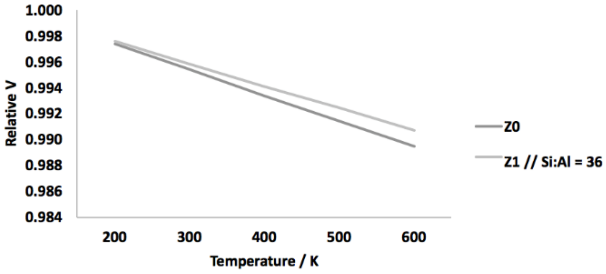

Figure 3. The variation of volume change as a function of the temperature. Z0 denominates the fully siliceous CHA framework structure and Z1 relates to the an Al substituted CHA structure, where the Al ions stand in the configuration seen in **Figure 2**.

The calculations predict this behaviour correctly for the purely siliceous case, but not for the Al substituted systems. As we see in **Table 2**, the ratio of the lattice parameters stays almost constant for each case. The same invariability was found with regards to the temperature; heating the system did not affect these ratios.

Taking into account that guest molecule hindrance and their diffusion rates affect the catalytic behaviour of certain catalysts, it is easy to imagine that, if the NTE did distort the framework enough, the catalytic behaviour would be modified. The more specific question is whether this applies to Cu/SSZ-13 in the *deNO*$_x$

Table 3 | A list of the computed CTEs of each system of the published literature.

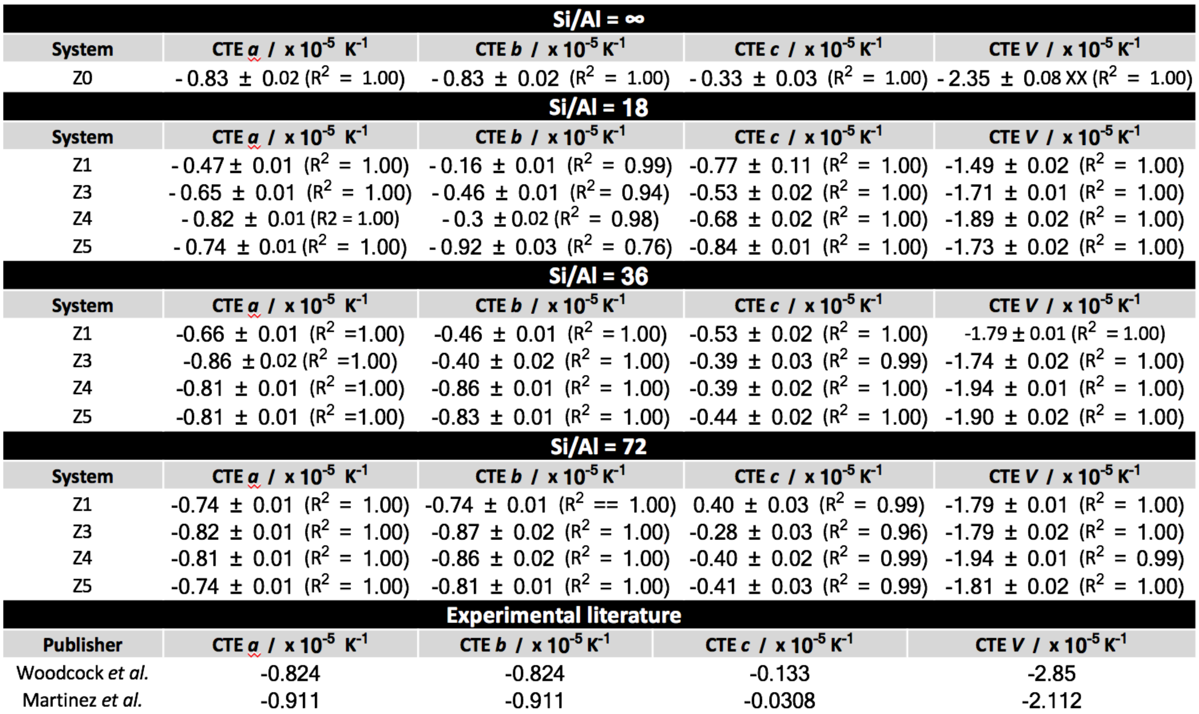

Si/Al = ∞				
System	**CTE *a* / x 10^{-5} K^{-1}**	**CTE *b* / x 10^{-5} K^{-1}**	**CTE *c* / x 10^{-5} K^{-1}**	**CTE *V* / x 10^{-5} K^{-1}**
Z0	- 0.83 ± 0.02 (R^2 = 1.00)	- 0.83 ± 0.02 (R^2 = 1.00)	- 0.33 ± 0.03 (R^2 = 1.00)	- 2.35 ± 0.08 XX (R^2 = 1.00)
Si/Al = 18				
System	**CTE *a* / x 10^{-5} K^{-1}**	**CTE *b* / x 10^{-5} K^{-1}**	**CTE *c* / x 10^{-5} K^{-1}**	**CTE *V* / x 10^{-5} K^{-1}**
Z1	- 0.47 ± 0.01 (R^2 = 1.00)	- 0.16 ± 0.01 (R^2 = 0.99)	-0.77 ± 0.11 (R^2 = 1.00)	-1.49 ± 0.02 (R^2 = 1.00)
Z3	- 0.65 ± 0.01 (R^2 = 1.00)	- 0.46 ± 0.01 (R^2 = 0.94)	-0.53 ± 0.02 (R^2 = 1.00)	-1.71 ± 0.01 (R^2 = 1.00)
Z4	- 0.82 ± 0.01 (R2 = 1.00)	- 0.3 ± 0.02 (R^2 = 0.98)	-0.68 ± 0.02 (R^2 = 1.00)	-1.89 ± 0.02 (R^2 = 1.00)
Z5	- 0.74 ± 0.01 (R^2 = 1.00)	- 0.92 ± 0.03 (R^2 = 0.76)	-0.84 ± 0.01 (R^2 = 1.00)	-1.73 ± 0.02 (R^2 = 1.00)
Si/Al = 36				
System	**CTE *a* / x 10^{-5} K^{-1}**	**CTE *b* / x 10^{-5} K^{-1}**	**CTE *c* / x 10^{-5} K^{-1}**	**CTE *V* / x 10^{-5} K^{-1}**
Z1	-0.66 ± 0.01 (R^2 =1.00)	-0.46 ± 0.01 (R^2 = 1.00)	-0.53 ± 0.02 (R^2 = 1.00)	-1.79 ± 0.01 (R^2 = 1.00)
Z3	-0.86 ± 0.02 (R^2 =1.00)	-0.40 ± 0.02 (R^2 = 1.00)	-0.39 ± 0.03 (R^2 = 0.99)	-1.74 ± 0.02 (R^2 = 1.00)
Z4	-0.81 ± 0.01 (R^2 =1.00)	-0.86 ± 0.01 (R^2 = 1.00)	-0.39 ± 0.02 (R^2 = 1.00)	-1.94 ± 0.01 (R^2 = 1.00)
Z5	-0.81 ± 0.01 (R^2 =1.00)	-0.83 ± 0.01 (R^2 = 1.00)	-0.44 ± 0.02 (R^2 = 1.00)	-1.90 ± 0.02 (R^2 = 1.00)
Si/Al = 72				
System	**CTE *a* / x 10^{-5} K^{-1}**	**CTE *b* / x 10^{-5} K^{-1}**	**CTE *c* / x 10^{-5} K^{-1}**	**CTE *V* / x 10^{-5} K^{-1}**
Z1	-0.74 ± 0.01 (R^2 = 1.00)	-0.74 ± 0.01 (R^2 == 1.00)	0.40 ± 0.03 (R^2 = 0.99)	-1.79 ± 0.01 (R^2 = 1.00)
Z3	-0.82 ± 0.01 (R^2 = 1.00)	-0.87 ± 0.02 (R^2 = 1.00)	-0.28 ± 0.03 (R^2 = 0.96)	-1.79 ± 0.02 (R^2 = 1.00)
Z4	-0.81 ± 0.01 (R^2 = 1.00)	-0.86 ± 0.02 (R^2 = 1.00)	-0.40 ± 0.02 (R^2 = 0.99)	-1.94 ± 0.01 (R^2 = 0.99)
Z5	-0.74 ± 0.01 (R^2 = 1.00)	-0.81 ± 0.01 (R^2 = 1.00)	-0.41 ± 0.03 (R^2 = 0.99)	-1.81 ± 0.02 (R^2 = 1.00)
Experimental literature				
Publisher	**CTE *a* / x 10^{-5} K^{-1}**	**CTE *b* / x 10^{-5} K^{-1}**	**CTE *c* / x 10^{-5} K^{-1}**	**CTE *V* / x 10^{-5} K^{-1}**
Woodcock *et al.*	-0.824	-0.824	-0.133	-2.85
Martinez *et al.*	-0.911	-0.911	-0.0308	-2.112

reaction? This is not fully answered by the current study. However, when zeolite powders are synthesised, the relative Al environments in the framework could be distorted enough that the Cu^{2+} could be deactivated and could reduce the conversion rates of NO_x. Further investigation in this matter ought to be made.

Conclusions

We have shown that different Al chemical environments, as well as different Al concentrations in the CHA framework, impact the NTE behaviour of Cu/SSZ-13. The presence of more Al ions in the zeolitic structure reduces the rate of contraction as a function of the temperature. The Cu extra-framework ion in the aluminous structures deviates slightly from the position where it is found in the purely siliceous form when heated. Since the zeolites used in many chemical applications have a wide range of concentration and types of Al environments, it is possible that a better understanding of how different chemical environments affect thermal behaviour (such as NTE) could promote the development of more efficient products, not only for the automotive industry but for zeolitic applications in general

Acknowledgments : DN is grateful to EPSRC and Johnson Matthey PLC for a studentship supported by the Molecular Modelling and Materials Science Centre for Doctoral Training.

References

1 M. Zaarour, B. Dong, I. Naydenova, R. Retoux and S. Mintova, *Microporous Mesoporous Mater.*, 2014, **189**, 11–21.
2 A. M. Beale, F. Gao, I. Lezcano-Gonzalez, C. H. F. Peden and J. Szanyi, *Chem. Soc. Rev.*, 2015, **44**, 7371–7405.
3 K. Leistner, A. Kumar, K.

Kamasamudram and L. Olsson, *Catal. Today*, 2016, 0–1.

4 W. Miller, C. W. Smith, D. S. MacKenzie and K. E. Evans, *J. Mater. Sci.*, 2009, **44**, 5441–5451.

5 A. Sleight, *Curr. Opin. Solid State Mater. Sci.*, 1998, **3**, 128–131.

6 D. Woodcock, P. Lightfoot, L. Villaescusa, M.-J. Diaz-Cabanas, M. Camblor and D. Engberg, *Chem. Mater.*, 1999, **11**, 2508–2514.

7 M. J. Sanders, M. Leslie and C. R. A. Catlow, *J. Chem. Soc. Chem. Commun.*, 1984, **4**, 1271.

8 C. R. A. Catlow, *Proc. R. Soc. A Math. Phys. Eng. Sci.*, 1977, **353**, 533–561.

9 G. Sastre, D. W. Lewis, C. Richard and A. Catlow, *J. Phys. Chem. B*, 1997, **101**, 5249–5262.

10 F. Göltl and P. Sautet, *J. Chem. Phys.*, 2014, **140**, 154105.

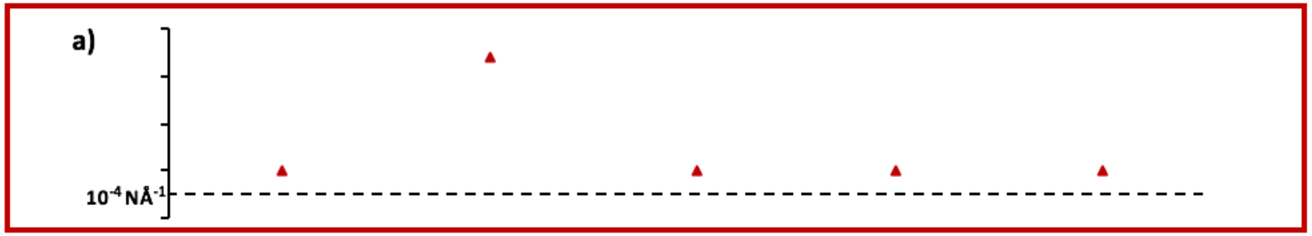
a)
10⁻⁴ NÅ⁻¹

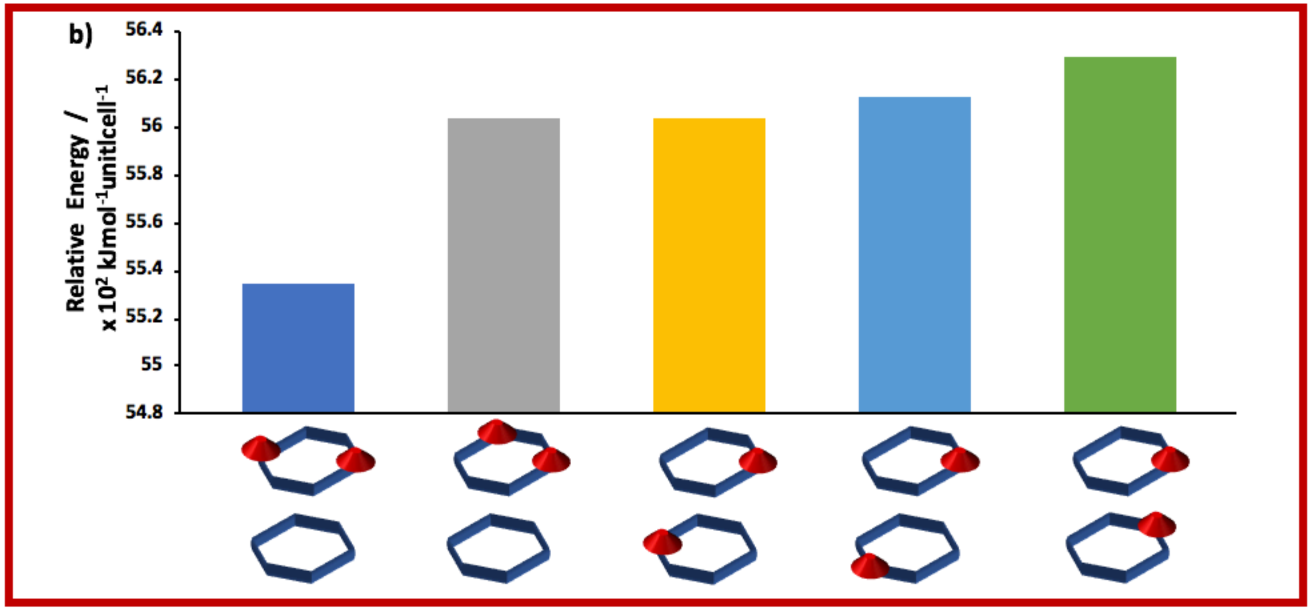
b)
Relative Energy /
x 10² kJmol⁻¹unitcell⁻¹
56.4
56.2
56
55.8
55.6
55.4
55.2
55
54.8